

Multipole ordering in f -electron systems on the basis of a j - j coupling scheme

Katsunori Kubo and Takashi Hotta

Advanced Science Research Center, Japan Atomic Energy Research Institute, Tokai, Ibaraki 319-1195, Japan

(Dated: February 8, 2020)

We investigate microscopic aspects of multipole ordering in f -electron systems with emphasis on the effect of lattice structure. For the purpose, first we construct f -electron models on three kinds of lattices, simple cubic (sc), bcc, and fcc, by including f -electron hopping through ($ff\sigma$) bonding in a tight-binding approximation on the basis of a j - j coupling scheme. Then, an effective model is derived in the strong-coupling limit for each lattice structure with the use of second-order perturbation theory with respect to ($ff\sigma$). By applying mean-field theory to such effective models, we find different types of multipole ordered state depending on the lattice structure. For the sc lattice, a Γ_{3g} antiferro-quadrupole transition occurs at a finite temperature and as further lowering temperature, we find another transition to a ferromagnetic state. For the bcc lattice, a Γ_{2u} antiferro-octupole ordering occurs first, and then, a ferromagnetic phase transition follows it. Finally, for the fcc lattice, we find a single phase transition to the longitudinal triple- q Γ_{5u} octupole ordering.

PACS numbers: 75.30.Et, 71.10.Fd, 75.40.Cx

I. INTRODUCTION

It is one of currently important issues in the research field of condensed matter physics to unveil exotic magnetic properties of strongly correlated electron materials with active orbital degree of freedom. Among those materials, in d -electron systems such as transition metal oxides, origin of complex magnetic structure has been vigorously discussed based on the concept of orbital ordering.^{1,2,3,4} Also in f -electron materials including rare-earth and actinide elements, various kinds of magnetic and orbital ordering have been found.^{5,6} It is now widely recognized that orbital degree of freedom plays a crucial role for the emergence of novel magnetism in d - and f -electron systems.

Here we should note that in f -electron systems, spin and orbital are not independent degrees of freedom, since they are tightly coupled with each other due to the strong spin-orbit interaction. Then, in order to describe such a complicated spin-orbital coupled system, we usually represent the f -electron state in terms of “multipole” degree of freedom, rather than using spin and orbital degrees of freedom as in d -electron systems. Among multipole moments, there have been intensive and extensive studies on dipole and/or quadrupole ordering in f -electron systems. In usual cases, magnetic ordering indicates dipole one, which can be detected by neutron diffraction experiments. Ordinary orbital ordering means quadrupole one, which can also be detected experimentally, since it induces lattice distortions due to the spatial anisotropy in charge distribution.

In addition to dipole and quadrupole ordering, in recent years, possibility of higher-order multipole ordering, i.e., magnetic octupole ordering, has been also discussed for $\text{Ce}_x\text{La}_{1-x}\text{B}_6$ ^{7,8,9,10,11,12,13} and NpO_2 ,^{14,15,16,17,18,19,20} to reconcile experimental observations which seem to contradict one another at first glance. Very recently, a possibility of octupole ordering has been proposed also for $\text{SmRu}_4\text{P}_{12}$.^{21,22} It is noted that in these mate-

rials, crystalline electric field (CEF) ground states are Γ_8 quartets with large degeneracy even under a CEF potential.^{23,24,25} In the Γ_8 ground-state multiplet, octupoles exist as independent moments besides dipole and quadrupole moments.²⁶ Then, phenomenological theories have been developed under the assumption that octupole ordering occurs. Note that direct detection of octupole ordering is very difficult, since the octupole moment directly couples to neither a magnetic field nor lattice distortions. However, those phenomenological theories have been successful in explaining several experimental facts consistently, e.g., induced quadrupole moments in octupole ordered states in $\text{Ce}_x\text{La}_{1-x}\text{B}_6$ ^{8,10} and NpO_2 .^{15,17}

As mentioned above, thus far, the study on multipole ordering in f -electron systems has been almost limited in the phenomenological level, mainly due to the complexity in the treatment of multipole degree of freedom. It might be possible to consider a Heisenberg-like model for multipole moments, but the interactions among multipole moments were determined just phenomenologically. It is highly required to proceed to microscopic theory, in order to understand the origin of multipole ordering in f -electron systems. However, it is very hard and practically impossible to study multipole ordering in the model retaining all the f -electron states. Then, it is necessary to consider a tractable model which keeps correct f -electron symmetry.

One way for such model construction is to use an LS coupling scheme. For instance, the Ruderman-Kittel-Kasuya-Yosida (RKKY) interactions were estimated in DyZn ,²⁷ and in CeB_6 and CeB_2C_2 ²⁸ from microscopic models using the LS coupling scheme. However, the method based on the LS coupling scheme is complicated and seems still hard to be extended. One reason for the difficulty is that we cannot apply standard quantum-field theoretical techniques in the LS coupling scheme, since Wick's theorem does not hold. From this viewpoint, it is recommended to use a j - j coupling scheme.²⁹ Since individual f -electron states are first defined, we can in-

clude many-body effects in systematic ways using theoretical techniques developed for the research of d -electron systems.^{20,29,30,31,32}

In this paper, in order to investigate how multipole ordering appears in f -electron systems from a microscopic viewpoint, we exploit the j - j coupling scheme. We construct tight-binding models on three kinds of lattices, simple cubic (sc), bcc, and fcc, by including Coulomb interactions among Γ_8 states. In order to discuss multipole ordering in these models, we derive an effective multipole interaction model in the strong-coupling limit for each lattice structure by using the second-order perturbation theory with respect to f - f hopping integrals, as to estimate the superexchange interaction in d -electron systems. Then, within a mean-field approximation, we clarify what kind of multipole ordering occurs in the effective model: For the sc lattice, a Γ_{3g} antiferro-quadrupole transition occurs, while for the bcc lattice, Γ_{2u} antiferro-octupole ordering appears. For the fcc lattice with geometrical frustration, we find longitudinal triple- \mathbf{q} Γ_{5u} octupole ordering.

The organization of this paper is as follows. In Sec. II, we introduce a tight-binding model based on the j - j coupling scheme including only the Γ_8 states. In Sec. III, we describe the general prescription to derive an effective Hamiltonian from the Γ_8 model. In Sec. IV, we show the mean-field results of the effective models on sc, bcc, and fcc lattices. Finally, in Sec. V, the paper is summarized.

II. HAMILTONIAN

In the j - j coupling scheme, we first include the spin-orbit interaction, and consider only the states with total angular momentum $j=5/2$. These $j=5/2$ states are further split into Γ_7 doublet and Γ_8 quartet due to a cubic CEF. In order to consider multipole phenomena such as octupole ordering in f -electron systems from a microscopic viewpoint, in this paper we consider only Γ_8 states by assuming large CEF splitting energy between Γ_7 and Γ_8 levels. This simplification is motivated by the fact that the possibility of exotic octupole ordering has been actively discussed in $\text{Ce}_x\text{La}_{1-x}\text{B}_6$ and NpO_2 with Γ_8 ground state.

Here readers may be doubtful of the reality of our assumption, since the Coulomb interaction among f electrons is naively thought to be larger than the CEF level splitting in any case. However, it should be noted that we are now considering the f -electron state in the j - j coupling scheme, not in the original f -electron state with angular momentum $\ell=3$. As pointed out in Ref. 29, the Hund's rule interaction in the j - j coupling scheme is effectively reduced to be 1/49 of the original Hund's rule coupling. Namely, even if the original Hund's rule coupling among f electrons is 1 eV, it is reduced to 200 K in the j - j coupling scheme. We note that the CEF level splitting in actinide dioxides is considered to be larger than 1000 K.^{20,33} We also recall that the CEF level split-

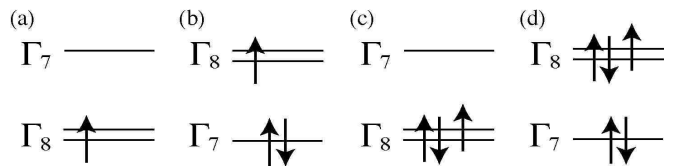


FIG. 1: Electron configurations in the j - j coupling scheme for Γ_8 CEF ground states. (a) One electron in the Γ_8 for $n=1$. (b) One electron in the Γ_8 for $n=3$. (c) One hole in the Γ_8 for $n=3$. (d) One hole in the Γ_8 for $n=5$.

ting in CeB_6 is as large as 500 K.²³ Thus, we safely conclude that our present assumption is correctly related to the realistic situation. Of course, in order to achieve quantitative agreement with experimental results, it is necessary to include also Γ_7 level, since the magnitude of the CEF splitting is always finite, even if it is large compared with the effective Hund's rule interaction. However, we strongly believe that it is possible to grasp microscopic origin of multipole ordering in f -electron systems on the basis of the Γ_8 model, since this model is considered to be connected adiabatically from the realistic situation. We postpone further effort to develop more general theory to include all the $j=5/2$ sextet in future.

Concerning the f -electron number, in this paper we treat only the case with one f electron in the Γ_8 multiplet per site. However, this restriction does *not* simply indicate that we consider only the Ce-based compound. In the j - j coupling scheme, in order to consider f^n -electron systems, where n indicates local f electron number per site, we accommodate f electrons in the one-electron CEF levels due to the balance between Coulomb interactions and CEF level splitting energy, just as in the case of d -electron systems. Thus, the situation with one f electron in the Γ_8 multiplet per site expresses both cases with $n=1$ in the Γ_8 - Γ_7 [Fig. 1(a)] and $n=3$ in the Γ_7 - Γ_8 [Fig. 1(b)] systems, where Γ_x - Γ_y symbolically denotes the situation with Γ_x ground and Γ_y excited states. Furthermore, we should note that due to the electron-hole symmetry in the Γ_8 subspace, the effective model with one f electron in the Γ_8 state is the same for that in the case with three electrons in the Γ_8 multiplet. Namely, the present model also indicates both cases with $n=3$ in the Γ_8 - Γ_7 [Fig. 1(c)] and $n=5$ in the Γ_7 - Γ_8 [Fig. 1(d)] systems.

Before proceeding to the exhibition of the Hamiltonian, it is necessary to define f -electron operators in Γ_8 states. Since the Γ_8 quartet consists of two Kramers doublets, we introduce orbital index τ ($=\alpha$ and β) to distinguish the two Kramers doublets, while spin index σ ($=\uparrow$ and \downarrow) is defined to distinguish the two states in each Kramers doublet. In the second-quantized form, annihilation operators for Γ_8 electrons are defined as

$$f_{\mathbf{r}\alpha\uparrow} = \sqrt{5/6}a_{\mathbf{r}5/2} + \sqrt{1/6}a_{\mathbf{r}-3/2}, \quad (1a)$$

$$f_{\mathbf{r}\alpha\downarrow} = \sqrt{5/6}a_{\mathbf{r}-5/2} + \sqrt{1/6}a_{\mathbf{r}3/2}, \quad (1b)$$

for α -orbital electrons, and

$$f_{\mathbf{r}\beta\uparrow} = a_{\mathbf{r}1/2}, \quad (2a)$$

$$f_{\mathbf{r}\beta\downarrow} = a_{\mathbf{r}-1/2}, \quad (2b)$$

for β -orbital electrons, where $a_{\mathbf{r}j_z}$ is the annihilation operator for an electron with the z -component j_z of the total angular momentum at site \mathbf{r} .

Now we show the Hamiltonian of Γ_8 electrons. For the purpose to consider the effective model later, it is convenient to express the Hamiltonian in the form of

$$\mathcal{H} = \mathcal{H}_{\text{kin}} + \mathcal{H}_{\text{loc}}, \quad (3)$$

where \mathcal{H}_{kin} denotes the kinetic term of f electrons and \mathcal{H}_{loc} indicates the local interaction part for Γ_8 electrons. In this paper, the kinetic term of Γ_8 electrons is given by exploiting the tight-binding approximation. Then, \mathcal{H}_{kin} is expressed as

$$\mathcal{H}_{\text{kin}} = \sum_{\mathbf{r}, \boldsymbol{\mu}, \tau, \sigma, \tau', \sigma'} t_{\tau\sigma; \tau'\sigma'}^{\boldsymbol{\mu}} f_{\mathbf{r}\tau\sigma}^\dagger f_{\mathbf{r}+\boldsymbol{\mu}\tau'\sigma'}, \quad (4)$$

where $\boldsymbol{\mu}$ is a vector connecting nearest-neighbor sites and $t_{\tau\sigma; \tau'\sigma'}^{\boldsymbol{\mu}}$ is the hopping integral of an electron with (τ', σ') at site $\mathbf{r}+\boldsymbol{\mu}$ to the (τ, σ) state at \mathbf{r} . We note that the hopping integral $t_{\tau\sigma; \tau'\sigma'}^{\boldsymbol{\mu}}$ depends on orbital, spin, and direction $\boldsymbol{\mu}$, due to f -electron symmetry. Then, the form of the hopping integral is characteristic of lattice structure. The explicit form of the hopping matrix will be shown later for each lattice structure. Note also the relation $t_{\tau\sigma; \tau'\sigma'}^{-\boldsymbol{\mu}} = t_{\tau\sigma; \tau'\sigma'}^{\boldsymbol{\mu}}$.

As for the local f -electron term \mathcal{H}_{loc} , since we assume the large CEF splitting energy between Γ_7 and Γ_8 levels, it is enough to consider the Coulomb interaction terms among Γ_8 electrons. As easily understood from the introduction of ‘spin’ and ‘orbital’ in the j - j coupling scheme, the local f -electron term in the Γ_8 quartet becomes the same as that of the two-orbital systems for d electrons. In fact, after lengthy algebraic calculations for Racah parameters in the j - j coupling scheme,²⁹ \mathcal{H}_{loc} is given as

$$\begin{aligned} \mathcal{H}_{\text{loc}} = & U \sum_{\mathbf{r}\tau} n_{\mathbf{r}\tau\uparrow} n_{\mathbf{r}\tau\downarrow} + U' \sum_{\mathbf{r}} n_{\mathbf{r}\alpha} n_{\mathbf{r}\beta} \\ & + J \sum_{\mathbf{r}, \sigma, \sigma'} f_{\mathbf{r}\alpha\sigma}^\dagger f_{\mathbf{r}\beta\sigma'}^\dagger f_{\mathbf{r}\alpha\sigma'} f_{\mathbf{r}\beta\sigma} \\ & + J' \sum_{\mathbf{r}, \tau \neq \tau'} f_{\mathbf{r}\tau\uparrow}^\dagger f_{\mathbf{r}\tau\downarrow}^\dagger f_{\mathbf{r}\tau'\downarrow} f_{\mathbf{r}\tau'\uparrow}, \end{aligned} \quad (5)$$

where $n_{\mathbf{r}\tau\sigma} = f_{\mathbf{r}\tau\sigma}^\dagger f_{\mathbf{r}\tau\sigma}$ and $n_{\mathbf{r}\tau} = \sum_{\sigma} n_{\mathbf{r}\tau\sigma}$. The coupling constants U , U' , J , and J' denote the intra-orbital Coulomb, inter-orbital Coulomb, exchange, and pair-hopping interactions, respectively. These are expressed in terms of Racah parameters, and we obtain the relation $U=U'+J+J'$, which can be understood from the rotational invariance in orbital space.²⁹ Note that for d -electron systems, one also has the relation $J=J'$. When

the electronic wave-function is real, this relation is easily demonstrated from the definition of the Coulomb integral. However, in the j - j coupling scheme the wave-function is complex, and J is not equal to J' in general.

III. EFFECTIVE MODEL

In this section, we describe a method to derive an effective Hamiltonian by using the second-order perturbation theory with respect to hopping integrals. When the Hamiltonian is written in the form of Eq. (3), first we solve the local problem

$$\mathcal{H}_{\text{loc}}|\Phi_n^a\rangle = E_n|\Phi_n^a\rangle, \quad (6)$$

where E_n denotes the n -th eigenenergy and $|\Phi_n^a\rangle$ is the corresponding eigenstate with a label a to distinguish the degenerate states. Since we accommodate one electron per site, the ground state $|\Phi_0^a\rangle$ is expressed as

$$|\Phi_0^a\rangle = \prod_{\mathbf{r}, \tau, \sigma} f_{\mathbf{r}\tau\sigma}^\dagger P_a(\mathbf{r}, \tau, \sigma) |0\rangle, \quad (7)$$

where $|0\rangle$ is the vacuum state of f electrons, a denotes the electron configuration in the ground state with one electron per site, and $P_a(\mathbf{r}, \tau, \sigma)$ takes 0 or 1 depending on the configuration a .

Here we consider the formal perturbation expansion in terms of \mathcal{H}_{kin} in order to construct the effective model. Within the second order, \mathcal{H}_{eff} is generally written as

$$\mathcal{H}_{\text{eff}} = \sum_{a,b,u} \sum_{m \neq 0} |\Phi_0^a\rangle \langle \Phi_0^a | \mathcal{H}_{\text{kin}} \frac{|\Phi_m^u\rangle \langle \Phi_m^u|}{E_0 - E_m} \mathcal{H}_{\text{kin}} |\Phi_0^b\rangle \langle \Phi_0^b|, \quad (8)$$

where a and b are labels to distinguish the ground states, while u is the label for the degenerate excited states.

Since we consider the situation with one electron per site, the intermediate state due to one-electron hopping has a vacant and a double occupied site. The double occupied site has six possible states, composed of Γ_5 triplet with energy $U'-J$, Γ_3 doublet with energy $U'+J(=U-J')$, and Γ_1 singlet with energy $U+J'$. For the mathematical completion, it is necessary to include all possible excited states in the intermediate process, but the calculation becomes complicated. Then, in this paper, in order to grasp the essential point of the Γ_8 model by avoiding tedious calculations, we include only the lowest-energy Γ_5 triplet among the intermediate f^2 states. This restriction to the intermediate states is validated, when J is much larger than the hopping energy of f electron. Since the f -electron hopping amplitude is considered to be small compared with J , even if we also include the hybridization with conduction electrons, this approximation is acceptable in f -electron systems.

Let us explain the prescription to derive the effective model in the present case. It is convenient to consider exchange processes of electrons between two sites, \mathbf{r} and

TABLE I: Multipole operators in the Γ_8 subspace.²⁶ The site label \mathbf{r} is suppressed in this Table for simplicity.

Γ_γ	$2u$	$3gu$	$3gv$	$4u1x$	$4u1y$	$4u1z$	$4u2x$	$4u2y$	$4u2z$	$5ux$	$5uy$	$5uz$	$5gx$	$5gy$	$5gz$
multipole operator X^{Γ_γ}	T_{xyz}	O_2^0	O_2^2	J_x^{4u1}	J_y^{4u1}	J_z^{4u1}	J_x^{4u2}	J_y^{4u2}	J_z^{4u2}	T_x^{5u}	T_y^{5u}	T_z^{5u}	O_{yz}	O_{zx}	O_{xy}
pseudospin representation	$\hat{\tau}^y$	$\hat{\tau}^z$	$\hat{\tau}^x$	$\hat{\sigma}^x$	$\hat{\sigma}^y$	$\hat{\sigma}^z$	$\hat{\eta}^+ \hat{\sigma}^x$	$\hat{\eta}^- \hat{\sigma}^y$	$\hat{\tau}^z \hat{\sigma}^z$	$\hat{\zeta}^+ \hat{\sigma}^x$	$\hat{\zeta}^- \hat{\sigma}^y$	$\hat{\tau}^x \hat{\sigma}^z$	$\hat{\tau}^y \hat{\sigma}^x$	$\hat{\tau}^y \hat{\sigma}^y$	$\hat{\tau}^y \hat{\sigma}^z$

\mathbf{r}' . Since we consider the situation with one f electron per site, the initial state $|\mathbf{r}s_1, \mathbf{r}'s_2\rangle$ is written as

$$|\mathbf{r}s_1, \mathbf{r}'s_2\rangle = f_{\mathbf{r}s_1}^\dagger f_{\mathbf{r}'s_2}^\dagger |0\rangle, \quad (9)$$

where s_1 and s_2 symbolically denote spin and orbital states for both electrons. Then, we move one electron from the site \mathbf{r}' to \mathbf{r} . As mentioned above, the intermediate f^2 states at the site \mathbf{r} is restricted only as the lowest-energy Γ_5 triplet states. Namely, the intermediated states should be expressed as $|u, \mathbf{r}\rangle$ with the label u to distinguish the triplet states, given by

$$|+1, \mathbf{r}\rangle = f_{\mathbf{r}\alpha\uparrow}^\dagger f_{\mathbf{r}\beta\uparrow}^\dagger |0\rangle, \quad (10a)$$

$$|0, \mathbf{r}\rangle = (f_{\mathbf{r}\alpha\uparrow}^\dagger f_{\mathbf{r}\beta\downarrow}^\dagger + f_{\mathbf{r}\alpha\downarrow}^\dagger f_{\mathbf{r}\beta\uparrow}^\dagger) |0\rangle / \sqrt{2}, \quad (10b)$$

$$|-1, \mathbf{r}\rangle = f_{\mathbf{r}\alpha\downarrow}^\dagger f_{\mathbf{r}\beta\downarrow}^\dagger |0\rangle. \quad (10c)$$

In order to obtain the effective model Eq. (8), it is enough to evaluate the inner product

$$P_{u;s,s'} = \langle \mathbf{r}, u | \mathbf{r}s, \mathbf{r}s' \rangle. \quad (11)$$

This quantity is explicitly given by $P_{+1;\alpha\uparrow\beta\uparrow}=1$, $P_{0;\alpha\uparrow\beta\downarrow}=1/\sqrt{2}$, and the other non-zero elements are given by $P_{u;s's} = -P_{u;ss'}$ and $P_{-u;\tau-\sigma\tau'-\sigma'} = P_{u;\tau\sigma\tau'\sigma'}$.

Then, by including the processes in which an electron at \mathbf{r} moves first, we obtain the effective Hamiltonian as

$$\mathcal{H}_{\text{eff}} = - \sum_{\langle \mathbf{r}, \mathbf{r}' \rangle} \sum_{s_1-s_4} I_{s_3, s_4; s_1, s_2}^{\mathbf{r}'-\mathbf{r}} f_{\mathbf{r}s_3}^\dagger f_{\mathbf{r}s_1} f_{\mathbf{r}'s_4}^\dagger f_{\mathbf{r}'s_2}, \quad (12)$$

where $\langle \mathbf{r}, \mathbf{r}' \rangle$ denotes the pair of nearest-neighbor sites and the generalized exchange interaction I is given by

$$I_{s_3, s_4; s_1, s_2}^{\mathbf{r}'-\mathbf{r}} = \sum_{u, s, s'} [(t_{s', s_4}^{\mathbf{r}'-\mathbf{r}})^* P_{u; s_3, s'}^* P_{u; s_1, s} t_{s, s_2}^{\mathbf{r}'-\mathbf{r}} + (t_{s', s_3}^{\mathbf{r}-\mathbf{r}'})^* P_{u; s_4, s'}^* P_{u; s_2, s} t_{s, s_1}^{\mathbf{r}-\mathbf{r}'}] / (U - J). \quad (13)$$

In order to investigate the multipole ordering, it is more convenient to express the effective Hamiltonian Eq. (12) in terms of multipole operators. For the purpose, we introduce some notations to describe multipole operators as

$$\tilde{1}_{\tau\sigma; \tau'\sigma'} \equiv \delta_{\tau\tau'} \delta_{\sigma\sigma'}, \quad (14a)$$

$$\tilde{\tau}_{\tau\sigma; \tau'\sigma'} \equiv \boldsymbol{\sigma}_{\tau\tau'} \delta_{\sigma\sigma'}, \quad (14b)$$

$$\tilde{\boldsymbol{\sigma}}_{\tau\sigma; \tau'\sigma'} \equiv \delta_{\tau\tau'} \boldsymbol{\sigma}_{\sigma\sigma'}, \quad (14c)$$

$$\tilde{\eta}^\pm \equiv (\pm\sqrt{3}\tilde{\tau}^x - \tilde{\tau}^z)/2, \quad (14d)$$

$$\tilde{\zeta}^\pm \equiv -(\tilde{\tau}^x \pm \sqrt{3}\tilde{\tau}^z)/2, \quad (14e)$$

where $\boldsymbol{\sigma}$ are the Pauli matrices. By using these notations, we define one-particle operators at site \mathbf{r} as

$$\hat{A}_{\mathbf{r}} \equiv \sum_{\tau\tau'\sigma\sigma'} f_{\mathbf{r}\tau\sigma}^\dagger \tilde{A}_{\tau\sigma; \tau'\sigma'} f_{\mathbf{r}\tau'\sigma'}, \quad (15)$$

where \tilde{A} is a 4×4 matrix. The multipole operators in the Γ_8 subspace are listed in Table I.

With the use of above multipole operators, the effective Hamiltonian is finally arranged in the form of

$$\mathcal{H}_{\text{eff}} = \sum_{\mathbf{q}} (\mathcal{H}_{1\mathbf{q}} + \mathcal{H}_{2\mathbf{q}} + \mathcal{H}_{4u1\mathbf{q}} + \mathcal{H}_{4u2\mathbf{q}}), \quad (16)$$

where \mathbf{q} is the wave vector and $\mathcal{H}_{1\mathbf{q}}$ denotes quadrupole interactions. $\mathcal{H}_{4un\mathbf{q}}$ ($n=1$ or 2) denotes interactions between Γ_{4un} moments and ones between Γ_{4un} and other octupole moments with symmetry different from Γ_{4u} . $\mathcal{H}_{2\mathbf{q}}$ denotes other dipole and octupole interactions. In general, $\mathcal{H}_{2\mathbf{q}}$ includes interactions between Γ_{4u1} and Γ_{4u2} moments, but we find that such interactions are not included in the models with hopping integrals only through $(ff\sigma)$ bonding on sc, bcc, and fcc lattices. The explicit form of each multipole interaction sensitively depends on the lattice structure, as shown in the next section.

IV. RESULTS

Now we can calculate the effective interaction between two electrons located along any direction $\mathbf{r}' - \mathbf{r}$ by using Eq. (13), if the hopping integral along this direction is determined. The hopping integrals of f electrons are evaluated by using the Slater-Koster table.³⁴ In this section, we consider the nearest-neighbor hopping integrals through $(ff\sigma)$ bonding for three lattice structures, sc, bcc, and fcc. Then, we present the effective Hamiltonian and its ordered states for each lattice. The structure of our effective model is consistent with the general form of nearest-neighbor multipole interactions on each lattice derived by Sakai *et al.*³⁵ We follow the notation in Ref. 35 for convenience.

A. sc lattice

The nearest-neighbor hopping integrals through $(ff\sigma)$ bonding for the sc lattice are given by

$$t^{(a,0,0)} = [\tilde{1} - \tilde{\eta}^+] t_1, \quad (17a)$$

$$t^{(0,a,0)} = [\tilde{1} - \tilde{\eta}^-] t_1, \quad (17b)$$

$$t^{(0,0,a)} = [\tilde{1} - \tilde{\tau}^z] t_1, \quad (17c)$$

TABLE II: Coupling constants in the effective model for the sc lattice. The energy unit is $(1/8)t_1^2/(U' - J)$.

a_1	b_6	$b_1^{(1)}$	$b_2^{(1)}$	$b_3^{(1)}$	$b_1^{(2)}$	$b_2^{(2)}$	$b_3^{(2)}$
12	3	-4	-4	0	4	1	$-\sqrt{3}$

where a is the lattice constant and $t_1=3(ff\sigma)/14$.

For the sc lattice, the quadrupole interaction term in Eq. (16) is given by

$$\mathcal{H}_{1\mathbf{q}} = a_1(O_{2,-\mathbf{q}}^0 O_{2,\mathbf{q}}^0 C_z + \text{c.p.}), \quad (18)$$

where c.p. denotes cyclic permutations and $C_\nu = \cos(q_\nu a)$ ($\nu=x, y, \text{ or } z$). The value of the coupling constant a_1 is given in Table II.

Note that $O_{2\mathbf{q}}^0$ transforms to $(\sqrt{3}O_{2\mathbf{q}}^2 - O_{2\mathbf{q}}^0)/2$ and $(-\sqrt{3}O_{2\mathbf{q}}^2 - O_{2\mathbf{q}}^0)/2$ under c.p. $(x, y, z) \rightarrow (y, z, x)$ and $(x, y, z) \rightarrow (z, x, y)$, respectively. The dipole and octupole interactions are given by

$$\mathcal{H}_{2\mathbf{q}} = b_6[T_{z,-\mathbf{q}}^{5u} T_{z,\mathbf{q}}^{5u} (C_x + C_y) + \text{c.p.}], \quad (19)$$

and

$$\begin{aligned} \mathcal{H}_{4un\mathbf{q}} = & b_1^{(n)} [J_{z-\mathbf{q}}^{4un} J_{z\mathbf{q}}^{4un} C_z + \text{c.p.}] \\ & + b_2^{(n)} [J_{z-\mathbf{q}}^{4un} J_{z\mathbf{q}}^{4un} (C_x + C_y) + \text{c.p.}] \\ & + b_3^{(n)} [T_{z-\mathbf{q}}^{5u} J_{z\mathbf{q}}^{4un} (C_x - C_y) + \text{c.p.}], \end{aligned} \quad (20)$$

where values of the coupling constants b_i and $b_i^{(n)}$ are shown in Table II.

Note that the form of the hopping integrals Eqs. (17) are exactly the same as those for the e_g orbitals of d electrons via $(dd\sigma)$ bonding.^{29,36} Thus, the effective Hamiltonian has the same form as in the e_g model considering only the lowest-energy intermediate states,³⁷ when we interpret that τ and σ denote e_g orbital and real spin, respectively. However, the physical meaning of the present model is different from that of the e_g model. In particular, the effect of a magnetic field is essentially different. The dipole moment which couples to a magnetic field \mathbf{H} is given by $\mathbf{J}=(7/6)[\mathbf{J}^{4u1}+(4/7)\mathbf{J}^{4u2}]$ for the Γ_8 model, while for the e_g model, real spin σ of d electrons is simply coupled to a magnetic field. In contrast to the e_g model, a magnetic field resolves the degeneracy in the τ space even within a mean-field theory for the present model, as we will see later.

By applying mean-field theory to the effective model, we find a Γ_{3g} antiferro-quadrupole transition at a temperature $T=T_{3g}=3a_1/k_B$. As lowering temperature further, we find a Γ_{4u1} ferromagnetic transition. This ferromagnetic transition can be regarded as a Γ_{5u} antiferro-octupole transition, since the Γ_{4u1} ferromagnetic state with the Γ_{3g} antiferro-quadrupole moment is equivalent to the Γ_{5u} antiferro-octupole ordered state with the Γ_{3g} antiferro-quadrupole moment. The ground state energy is $(-3/2)a_1 - 2b_6 + b_1^{(1)} + 2b_2^{(1)}$ per site.

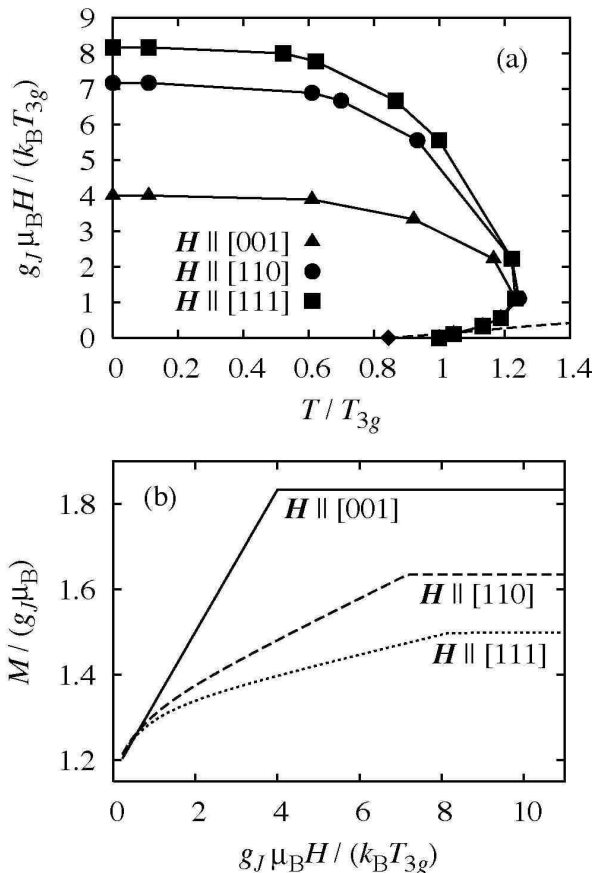


FIG. 2: Phase diagram and magnetization for the sc lattice. The Landé g -factor is $g_J=6/7$. (a) H - T phase diagram for three magnetic field directions. Solid symbols denote the Γ_{3g} quadrupole transition. The diamond represents the ferromagnetic transition point. The dashed curve represents the crossover to the ferromagnetic state. The definition of the crossover is given in the main text. (b) Magnetization as a function of magnetic field.

In Fig. 2(a), we depict an H - T phase diagram. We note that the ferromagnetic transition at zero magnetic field turns to be a crossover under the finite magnetic field. The crossover is drawn by dashed curve, determined by the peak position in the magnetic susceptibility. Since it is found that the crossover curve is almost isotropic in the region shown here, we depict only the curve for $\mathbf{H} \parallel [001]$. Note also that under a magnetic field, Γ_{4u1} moments become finite, and then, the Γ_{5u} antiferro-octupole interaction ($b_6 > 0$) effectively becomes a Γ_{3g} antiferro-quadrupole interaction. Thus, the Γ_{3g} antiferro-quadrupole transition temperature increases as H is increased at a low magnetic field region. This behavior reminds us of the experimental results for CeB_6 , although the order parameter in the quadrupole ordered phase of CeB_6 is the Γ_{5g} quadrupole moment. Magnetization as a function of H is shown in Fig. 2(b). The magnetization is isotropic as $H \rightarrow 0$ since the Γ_{4u1} moment is isotropic, while anisotropy develops under a high

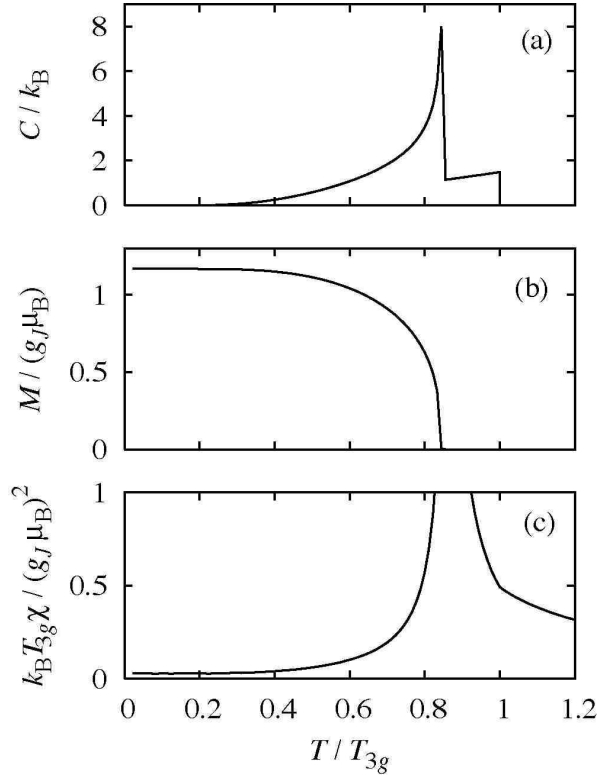


FIG. 3: Temperature dependence of physical quantities in the absence of magnetic field for the bcc lattice. (a) Specific heat. (b) Magnetization. (c) Magnetic susceptibility.

magnetic field.

In Figs. 3(a)–(c), we show specific heat, magnetization, and magnetic susceptibility, respectively, as functions of temperature. We observe two-step jump of specific heat at the quadrupole and ferromagnetic transition temperatures, since we have applied the mean-field theory to these second-order transitions. Note that the magnetization starts to develop below the ferromagnetic transition temperature. The magnetic susceptibility exhibits a bend at T_{3g} , while it diverges at the ferromagnetic transition temperature. Under the magnetic field, this divergence turns to be a peak, which defines the crossover to the ferromagnetic state in the H - T phase diagram.

Without magnetic field, the orbital (τ) state is continuously degenerate in the mean-field theory, although such continuous symmetry is absent in this model. As has been discussed for an e_g electron model such as perovskite manganites,³⁸ quantum fluctuations can resolve this continuous degeneracy, but in the present model with the strong spin-orbit interaction, magnetic field can resolve this degeneracy. The ground states are ferromagnetic with $\langle \mathbf{J}^{Au1} \rangle \parallel \mathbf{H}$, where $\langle \dots \rangle$ denotes the expectation value. Accompanied O_2^2 ordering is G-type [$\mathbf{q} = (1/2, 1/2, 1/2)$ in units of $2\pi/a$] or C-type [$\mathbf{q} = (1/2, 1/2, 0)$] for $\mathbf{H} \parallel [001]$, while for $\mathbf{H} \parallel [110]$, it is C-type. For $\mathbf{H} \parallel [111]$, there appear C-type O_2^2 ordering or equivalent ones in the cubic symmetry.

TABLE III: Coupling constants in the effective model for the bcc lattice. The energy unit is $(882/1327)t_2^2/(U' - J)$.

a_3	a_4	b_5	b_6	b_7	$b_1^{(1)}$	$b_2^{(1)}$	$b_3^{(1)}$	$b_4^{(1)}$	$b_1^{(2)}$	$b_2^{(2)}$	$b_3^{(2)}$	$b_4^{(2)}$
1	-2	9	2	2	-1	2	$-2\sqrt{3}$	0	2	2	0	$-2\sqrt{3}$

B. bcc lattice

The hopping integrals for the bcc lattice are given by

$$t^{(a/2, a/2, a/2)} = [\tilde{1} + \tilde{\tau}^y(\tilde{\sigma}^x + \tilde{\sigma}^y + \tilde{\sigma}^z)/\sqrt{3}]t_2, \quad (21a)$$

$$t^{(-a/2, a/2, a/2)} = [\tilde{1} + \tilde{\tau}^y(\tilde{\sigma}^x - \tilde{\sigma}^y - \tilde{\sigma}^z)/\sqrt{3}]t_2, \quad (21b)$$

$$t^{(a/2, -a/2, a/2)} = [\tilde{1} + \tilde{\tau}^y(-\tilde{\sigma}^x + \tilde{\sigma}^y - \tilde{\sigma}^z)/\sqrt{3}]t_2, \quad (21c)$$

$$t^{(a/2, a/2, -a/2)} = [\tilde{1} + \tilde{\tau}^y(-\tilde{\sigma}^x - \tilde{\sigma}^y + \tilde{\sigma}^z)/\sqrt{3}]t_2, \quad (21d)$$

where a is the lattice constant and $t_2 = 2(ff\sigma)/21$.

After some algebraic calculations, we obtain the quadrupole interaction term for the bcc lattice as

$$\mathcal{H}_{1\mathbf{q}} = a_3(O_{xy, -\mathbf{q}}O_{xy, \mathbf{q}} + \text{c.p.})c_x c_y c_z + a_4[O_{yz, -\mathbf{q}}O_{yz, \mathbf{q}}s_x s_y c_z + \text{c.p.}]. \quad (22)$$

The dipole and octupole interactions are given by

$$\begin{aligned} \mathcal{H}_{2\mathbf{q}} = & b_5 T_{xyz, -\mathbf{q}} T_{xyz, \mathbf{q}} c_x c_y c_z \\ & + b_6 (T_{z, -\mathbf{q}}^{5u} T_{z, \mathbf{q}}^{5u} + \text{c.p.}) c_x c_y c_z \\ & + b_7 [T_{x, -\mathbf{q}}^{5u} T_{y, \mathbf{q}}^{5u} s_x s_y c_z + \text{c.p.}], \end{aligned} \quad (23)$$

and

$$\begin{aligned} \mathcal{H}_{4un\mathbf{q}} = & b_1^{(n)} (J_{z-\mathbf{q}}^{4un} J_{z\mathbf{q}}^{4un} + \text{c.p.}) c_x c_y c_z \\ & + b_2^{(n)} [J_{x-\mathbf{q}}^{4un} J_{y\mathbf{q}}^{4un} s_x s_y c_z + \text{c.p.}] \\ & + b_3^{(n)} T_{xyz-\mathbf{q}} (J_{z\mathbf{q}}^{4un} s_x s_y c_z + \text{c.p.}) \\ & + b_4^{(n)} [T_{z-\mathbf{q}}^{5u} (-J_{x\mathbf{q}}^{4un} s_z s_x c_y + J_{y\mathbf{q}}^{4un} s_y s_z c_x) + \text{c.p.}], \end{aligned} \quad (24)$$

where $c_\nu = \cos(q_\nu a/2)$ and $s_\nu = \sin(q_\nu a/2)$. The values of the coupling constants a_i , b_i , and $b_i^{(n)}$ are shown in Table III.

In the mean-field approximation, we find a Γ_{2u} antiferro-octupole transition at $T_{2u} = 2b_5/k_B$ with $\mathbf{q} = (1, 0, 0)$, and a Γ_{4u1} ferromagnetic transition at a lower temperature. The ground state has the Γ_{5g} antiferro-quadrupole moment with the same ordering wave-vector as the Γ_{2u} moment. The ground state energy is $-a_3 - b_5 + b_1^{(1)}$ per site.

In Fig. 4(a), we show an H - T phase diagram. Again the ferromagnetic transition becomes a crossover under the finite magnetic field. The crossover curve determined by the peak in the magnetic susceptibility is found to be almost isotropic in the region shown here. Then, we show only the curve for $\mathbf{H} \parallel [001]$. In the region for high H and low T , we find two uniform phases. One is a phase with

uniform $\langle T_{xyz\mathbf{r}} \rangle$ depending on temperature and another is a phase with uniform $\langle T_{xyz\mathbf{r}} \rangle$ which does not depend on temperature, as shown in Figs. 4(a) and (c).

In Fig. 4(b), we show magnetization as a function of H . We note that the magnetization is isotropic as $H \rightarrow 0$ as in the sc lattice, since the order parameter of the ferromagnetic transition is the Γ_{4u1} moment. Note also that the jump in the magnetization at $(g_J \mu_B H)/(k_B T_{2u}) = 5.4$ for $\mathbf{H} \parallel [111]$ indicates the transition to the uniform state.

Figures 5(a)–(c) show specific heat, magnetization and magnetic susceptibility as functions of temperature, respectively. We observe two jumps in the specific heat at the octupole and ferromagnetic transition temperatures. The magnetization begins to develop below the ferromagnetic transition temperature. The magnetic susceptibility has a bend at T_{2u} and diverges at the ferromagnetic transition temperature. Note that the anomaly in the magnetic susceptibility at T_{2u} is very weak. In the pure magnetic Γ_{2u} octupole ordered state, there remains degeneracy, while in ordinary magnetic states, degeneracy is fully resolved. Thus, the nature of the Γ_{2u} octupole phase is similar to that of the quadrupole ordered phases. For instance, the anomaly in the magnetic susceptibility is weak at the transition temperature, there is no ordered magnetic dipole moment, and another phase transition occurs at a lower temperature.

The ground state is continuously degenerate, since the Γ_{4u1} and Γ_{5g} moments are isotropic in this model within the $\mathbf{q} = (1, 0, 0)$ structure. We note that this degeneracy is due to the symmetry of the model in contrast to the sc lattice. By applying a magnetic field, the ground states are uniquely determined. The ground states are ferromagnetic phases $\langle \mathbf{J}^{4u1} \rangle \parallel \mathbf{H}$ with antiferro O_{xy} ordering for $\mathbf{H} \parallel [001]$, with antiferro $O_{yz} + O_{zx}$ ordering for $\mathbf{H} \parallel [110]$, and with antiferro $O_{yz} + O_{zx} + O_{xy}$ ordering for $\mathbf{H} \parallel [111]$.

As mentioned in Sec. I, quite recently, a possibility of octupole ordering in filled skutterudite compound $\text{SmRu}_4\text{P}_{12}$ has been suggested experimentally.^{21,22} In the filled skutterudite structure, rare-earth ion surrounded by pnictogens form the bcc lattice. Moreover, the Γ_8 CEF ground state has been reported in the Sm-based filled skutterudite.²⁵ Thus, we expect to apply the present model to Sm-based filled skutterudites. When we compare our result on the bcc lattice with the experimental suggestion, octupole ordering actually occurs in our model for the bcc lattice, but Γ_{2u} octupole ordered state does not seem to explain the experimental results. This discrepancy is due to the suppression of Γ_7 orbital, since in the filled skutterudites, conduction electron has a_u symmetry, which hybridizes with Γ_7 electron. In addition, the level splitting between Γ_7 and Γ_8 is considered to be rather small in filled skutterudites. Thus, for filled-skutterudite materials, we should consider the $j=5/2$ sextet model in the bcc lattice with itinerant Γ_7 and localized Γ_8 orbitals. We postpone the analysis of such a model in future.

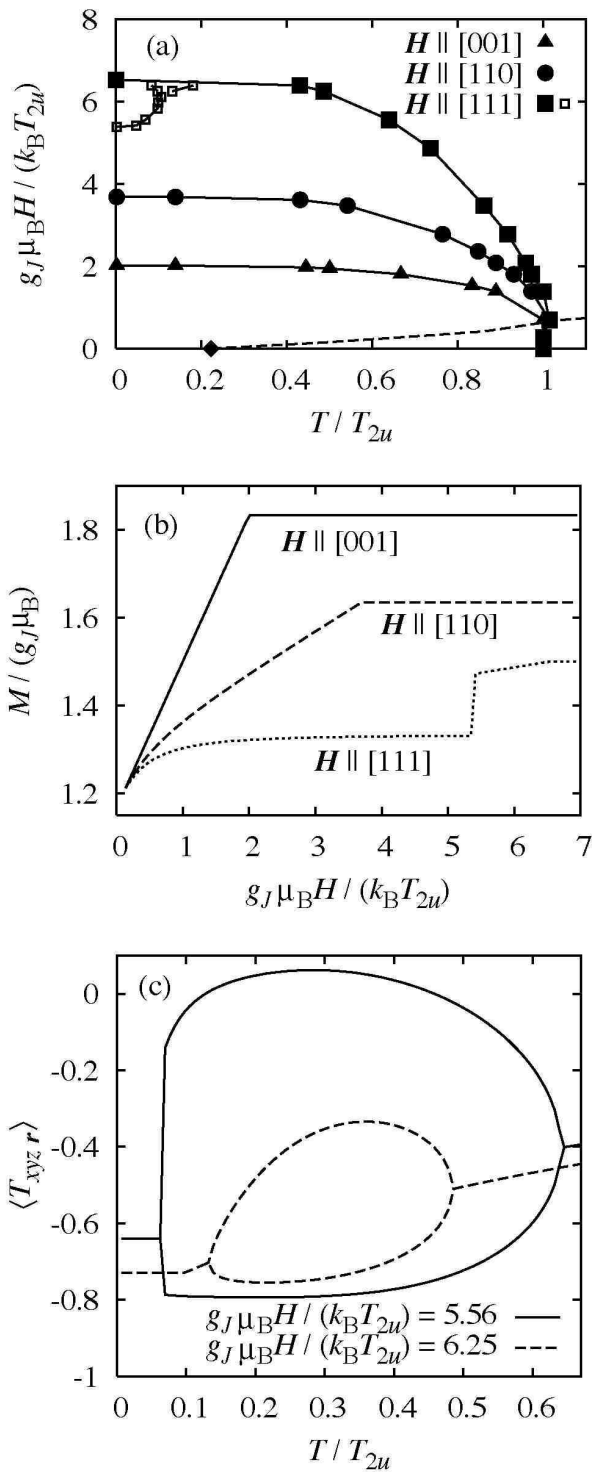


FIG. 4: (a) H - T phase diagram for the bcc lattice for three magnetic field directions. Solid symbols denote the Γ_{2u} octupole transition. The diamond represents the ferromagnetic transition point. The dashed curve represents the crossover to the ferromagnetic state. As for the definition of the crossover, see the main text. Open rectangles for $\mathbf{H} \parallel [111]$ denote transitions to uniform phases, as shown in (c). (b) Magnetization as a function of magnetic field for the bcc lattice. (c) Expectation value of Γ_{2u} octupole moment $\langle T_{xyz\mathbf{r}} \rangle$ at each of sublattice sites $\mathbf{r} = (0, 0, 0)$ and $(a/2, a/2, a/2)$ under high magnetic fields along $[111]$ for the bcc lattice.

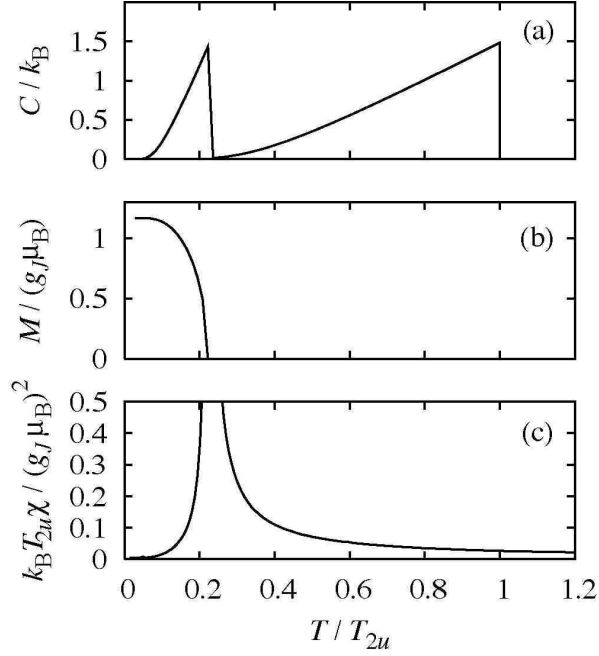


FIG. 5: Temperature dependence of physical quantities in the absence of magnetic field for the bcc lattice. (a) Specific heat. (b) Magnetization. (c) Magnetic susceptibility.

C. fcc lattice

The hopping integrals for the fcc lattice are given by

$$t^{(0,a/2,a/2)} = [\tilde{1} + (\tilde{\eta}^+ - 4\sqrt{3}\tilde{\tau}^y\tilde{\sigma}^x)/7]t_3, \quad (25a)$$

$$t^{(a/2,0,a/2)} = [\tilde{1} + (\tilde{\eta}^- - 4\sqrt{3}\tilde{\tau}^y\tilde{\sigma}^y)/7]t_3, \quad (25b)$$

$$t^{(a/2,a/2,0)} = [\tilde{1} + (\tilde{\tau}^z - 4\sqrt{3}\tilde{\tau}^y\tilde{\sigma}^z)/7]t_3, \quad (25c)$$

$$t^{(0,a/2,-a/2)} = [\tilde{1} + (\tilde{\eta}^+ + 4\sqrt{3}\tilde{\tau}^y\tilde{\sigma}^x)/7]t_3, \quad (25d)$$

$$t^{(-a/2,0,a/2)} = [\tilde{1} + (\tilde{\eta}^- + 4\sqrt{3}\tilde{\tau}^y\tilde{\sigma}^y)/7]t_3, \quad (25e)$$

$$t^{(a/2,-a/2,0)} = [\tilde{1} + (\tilde{\tau}^z + 4\sqrt{3}\tilde{\tau}^y\tilde{\sigma}^z)/7]t_3, \quad (25f)$$

where a is the lattice constant and $t_3 = (f f \sigma)/8$.

Each multipole interaction term in the effective Hamiltonian for the fcc lattice is given by

$$\begin{aligned} \mathcal{H}_{1\mathbf{q}} = & a_1(O_{2,-\mathbf{q}}^0 O_{2,\mathbf{q}}^0 c_x c_y + \text{c.p.}) \\ & + a_3(O_{2,-\mathbf{q}}^0 O_{xy,\mathbf{q}} s_x s_y + \text{c.p.}) \\ & + a_4(O_{xy,-\mathbf{q}} O_{xy,\mathbf{q}} c_x c_y + \text{c.p.}), \end{aligned} \quad (26)$$

$$\begin{aligned} \mathcal{H}_{2\mathbf{q}} = & b_8 [T_{z,-\mathbf{q}}^{5u} T_{z,\mathbf{q}}^{5u} (c_y c_z + c_z c_x) + \text{c.p.}] \\ & + b_9 [T_{x,-\mathbf{q}}^{5u} T_{y,\mathbf{q}}^{5u} s_x s_y + \text{c.p.}] \\ & + b_{10} T_{xyz,-\mathbf{q}} T_{xyz,\mathbf{q}} (c_x c_y + \text{c.p.}), \end{aligned} \quad (27)$$

TABLE IV: Coupling constants in the effective model for the fcc lattice. The energy unit is $(1/196)t_3^2/(U' - J)$.

a_1	a_3	a_4	b_8	b_9	b_{10}	$b_1^{(1)}$	$b_2^{(1)}$	$b_3^{(1)}$
12	$64\sqrt{3}$	192	195	-336	576	-196	-4	0
$b_4^{(1)}$	$b_5^{(1)}$	$b_6^{(1)}$	$b_1^{(2)}$	$b_2^{(2)}$	$b_3^{(2)}$	$b_4^{(2)}$	$b_5^{(2)}$	$b_6^{(2)}$
$224\sqrt{3}$	0	0	4	193	-336	$64\sqrt{3}$	$2\sqrt{3}$	$112\sqrt{3}$

and

$$\begin{aligned} \mathcal{H}_{4un\mathbf{q}} = & b_1^{(n)} [J_{z-\mathbf{q}}^{4un} J_{z\mathbf{q}}^{4un} c_x c_y + \text{c.p.}] \\ & + b_2^{(n)} [J_{z-\mathbf{q}}^{4un} J_{z\mathbf{q}}^{4un} (c_y c_z + c_z c_x) + \text{c.p.}] \\ & + b_3^{(n)} [J_{x-\mathbf{q}}^{4un} J_{y\mathbf{q}}^{4un} s_x s_y + \text{c.p.}] \\ & + b_4^{(n)} [T_{xyz-\mathbf{q}} (J_{z\mathbf{q}}^{4un} s_x s_y + \text{c.p.})] \\ & + b_5^{(n)} [T_{z-\mathbf{q}}^{5u} J_{z\mathbf{q}}^{4un} c_z (c_x - c_y) + \text{c.p.}] \\ & + b_6^{(n)} [T_{z-\mathbf{q}}^{5u} (-J_{x\mathbf{q}}^{4un} s_z s_x + J_{y\mathbf{q}}^{4un} s_y s_z) + \text{c.p.}]. \end{aligned} \quad (28)$$

The values of the coupling constants a_i , b_i and $b_i^{(n)}$ are shown in Table IV.

As already mentioned in Ref. 20, it is necessary to analyze the effective model carefully for the fcc lattice, since the model includes geometrical frustration. It is risky to apply directly the mean-field approximation to the effective model. First we evaluate the correlation function in the ground state using an unbiased method such as exact diagonalization on the N -site lattice. Here we set $N=8$, as shown in Fig. 6(a). The correlation function of the multipole operators is given by

$$\chi_{\mathbf{q}}^{\Gamma_\gamma} = (1/N) \sum_{\mathbf{r},\mathbf{r}'} e^{i\mathbf{q}\cdot(\mathbf{r}-\mathbf{r}')} \langle X_{\mathbf{r}}^{\Gamma_\gamma} X_{\mathbf{r}'}^{\Gamma_\gamma} \rangle, \quad (29)$$

where $\langle \dots \rangle$ denotes the expectation value using the ground-state wave-function.

In Fig. 6 (b), we show results for the correlation functions. The interaction between Γ_{2u} moments (b_{10}) is large, but the correlation function of the Γ_{2u} moment is not enhanced, indicating that the frustration effect is significant for an Ising-like moment such as Γ_{2u} . We find large values of correlation functions for J_z^{4u2} , T_z^{5u} , and O_{xy} moments at $\mathbf{q}=(0,0,1)$. However, there is no term in the effective model which stabilizes O_{xy} quadrupole order at $\mathbf{q}=(0,0,1)$. We note that either of Γ_{4u2} and Γ_{5u} ordered states can accompany Γ_{5g} quadrupole moments. Thus, the enhancement of O_{xy} correlation function indicates an induced quadrupole moment in Γ_{4u2} or Γ_{5u} moment ordered states. Namely, the relevant interactions are $b_2^{(2)}$ and b_8 , which stabilize the J_z^{4u2} and T_z^{5u} order, respectively, at $\mathbf{q}=(0,0,1)$.

Next we study the ordered state by applying mean-field theory to the simplified model including only $b_2^{(2)}$ and b_8 . Since the coupling constant b_8 is slightly larger than

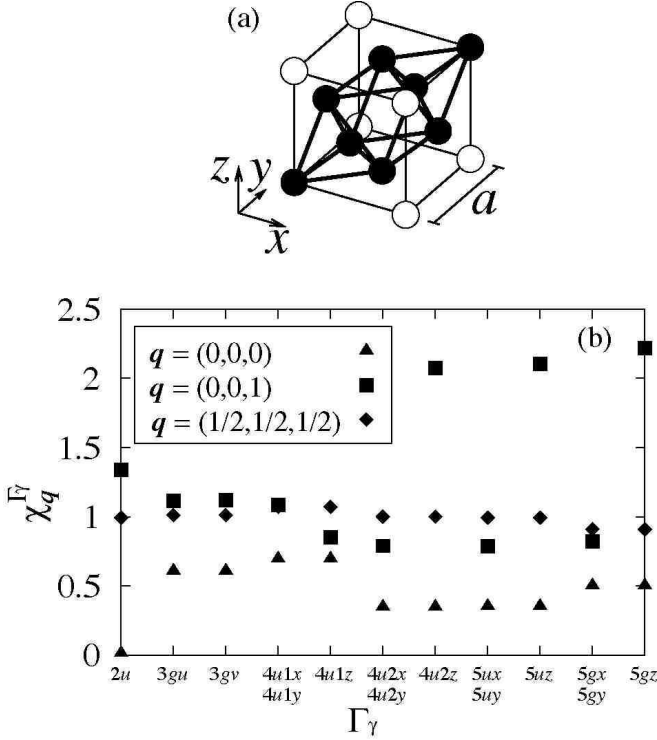


FIG. 6: (a) 8-site cluster (solid spheres) on the fcc lattice taken in the calculation. (b) Correlation functions for the 8-site cluster. The unit of the wave vectors is $2\pi/a$.

$b_2^{(2)}$, Γ_{5u} ordered state should have lower energy than Γ_{4u2} ordered state. The interaction b_8 stabilizes longitudinal ordering of the Γ_{5u} moments, i.e., $\langle \mathbf{T}_r^{5u} \rangle \parallel \mathbf{q}$.

However, we cannot conclude that the ground state is the single- \mathbf{q} state ($\langle T_{xr}^{5u} \rangle, \langle T_{yr}^{5u} \rangle, \langle T_{zr}^{5u} \rangle$) $\propto (0, 0, \exp[i2\pi z/a])$, since there is a possibility of multi- \mathbf{q} structures. For isotropic moments, single- \mathbf{q} and multi- \mathbf{q} structures have the same energy, and thus, anisotropy in the moment is important to determine the stable structure. Indeed, the Γ_{5u} moment has an easy axis along [111] in the Γ_8 subspace.^{10,17} In this case, we find that a triple- \mathbf{q} state is most stable among the single- \mathbf{q} and multi- \mathbf{q} states, since it gains interaction energy in all the directions.

In fact, the mean-field ground-state of the simplified model is the longitudinal triple- \mathbf{q} Γ_{5u} octupole state with four sublattices, i.e.,

$$\langle T_{xr}^{5u} \rangle \propto \exp[i2\pi x/a], \quad (30a)$$

$$\langle T_{yr}^{5u} \rangle \propto \exp[i2\pi y/a], \quad (30b)$$

$$\langle T_{zr}^{5u} \rangle \propto \exp[i2\pi z/a]. \quad (30c)$$

This state accompanies the triple- \mathbf{q} quadrupole moment¹⁵

$$\langle O_{yzt} \rangle \propto \langle T_{xr}^{5u} \rangle, \quad (31a)$$

$$\langle O_{zxt} \rangle \propto \langle T_{yr}^{5u} \rangle, \quad (31b)$$

$$\langle O_{xyt} \rangle \propto \langle T_{zr}^{5u} \rangle. \quad (31c)$$

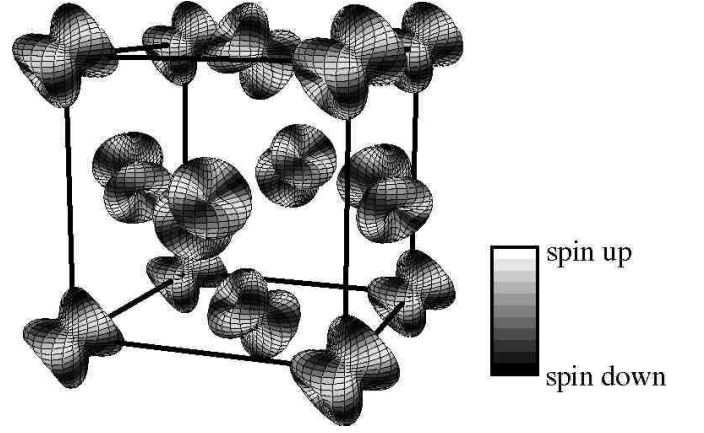


FIG. 7: The triple- \mathbf{q} Γ_{5u} octupole state. The surface is defined by $r = [\sum_{\sigma} |\psi(\theta, \phi, \sigma)|^2]^{1/2}$ in the polar coordinates, when the $5f$ wave-function is represented by $\Psi(r, \theta, \phi, \sigma) = R(r)\psi(\theta, \phi, \sigma)$, where σ denotes real spin. White-shift of the surface indicates the increase of the weight of up-spin state $|\psi(\theta, \phi, \uparrow)|^2/r^2$.

In Fig. 7, we show symmetry of the charge distribution with spin density in the triple- \mathbf{q} Γ_{5u} octupole state. Note that this triple- \mathbf{q} structure does not have frustration even in the fcc lattice. The ground state energy is $-4b_8$ per site, and the transition temperature is given by $k_B T_{5u} = 4b_8$. We also note that this triple- \mathbf{q} Γ_{5u} octupole state has been proposed for NpO_2 phenomenologically.¹⁵

Let us now evaluate physical quantities in the mean-field theory. Figures 8(a) and (b) show an H - T phase diagram and the magnetic field dependence of the magnetization at $T=0$, respectively. Note that the magnetization is isotropic as $H \rightarrow 0$ due to the cubic symmetry. The bend for $\mathbf{H} \parallel [001]$ and the dip for $\mathbf{H} \parallel [110]$ in magnetization indicate transitions to the two-sublattice structures. There is an anomaly in magnetization also for $\mathbf{H} \parallel [111]$ at the transition to the different sublattice structure, but it is very weak.

Under a high magnetic field, sublattice structures change, as shown in Fig. 9: For $\mathbf{H} \parallel [001]$, we obtain a two-sublattice structure with

$$\langle T_{xr}^{5u} \rangle = 0, \quad (32a)$$

$$\langle T_{yr}^{5u} \rangle = 0, \quad (32b)$$

$$\langle T_{zr}^{5u} \rangle \propto \exp[i2\pi z/a]. \quad (32c)$$

For $\mathbf{H} \parallel [110]$, there appears a two-sublattice structure with

$$\langle T_{xr}^{5u} \rangle \neq 0, \quad (33a)$$

$$\langle T_{yr}^{5u} \rangle \neq 0, \quad (33b)$$

$$\langle T_{zr}^{5u} \rangle = 0. \quad (33c)$$

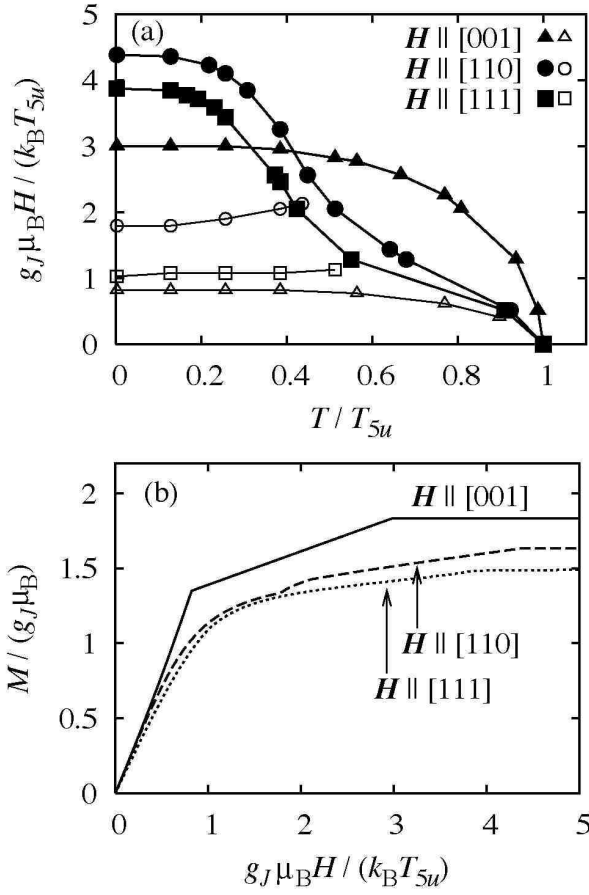


FIG. 8: Phase diagram and magnetization for the simplified model on the fcc lattice. (a) H - T phase diagram. Solid symbols denote the Γ_{5u} octupole transition, while open symbols denote transitions between Γ_{5u} octupole ordered states with different sublattice structures (see Fig. 9). (b) Magnetic field dependence of the magnetization.

Finally, for $\mathbf{H} \parallel [111]$, we observe

$$\langle T_{x\mathbf{r}}^{5u} \rangle \propto \sin[2\pi(y-z)/a], \quad (34a)$$

$$\langle T_{y\mathbf{r}}^{5u} \rangle \propto \sin[2\pi(z-x)/a], \quad (34b)$$

$$\langle T_{z\mathbf{r}}^{5u} \rangle \propto \sin[2\pi(x-y)/a]. \quad (34c)$$

Note also that the triple- \mathbf{q} state is fragile under $\mathbf{H} \parallel [110]$: $\langle T_{z\mathbf{r}}^{5u} \rangle = 0$ with a four-sublattice structure for $g_J \mu_B H / (k_B T_{5u}) \gtrsim 0.11$ at $T=0$ [this phase boundary is not shown in Fig. 8(a)].

Figures 10(a) and 10(b) show the temperature dependence of the specific heat and magnetic susceptibility, respectively. At $T=T_{5u}$, there appear the specific heat jump and a cusp in the magnetic susceptibility. In contrast to the sc and bcc lattices, there occurs single phase transition at zero magnetic field in the case of the fcc lattice. Note also that the cusp structure in the magnetic susceptibility is rather strong compared with experimental results.^{20,39} Such a quantitative disagreement with experiments is considered to originate from the suppres-

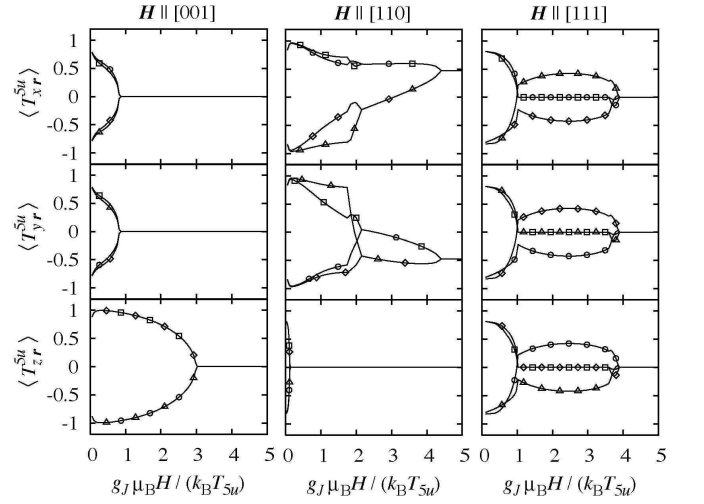


FIG. 9: Magnetic field dependence of Γ_{5u} octupole moments at $T=0$ at each of four-sublattice sites: $\mathbf{r}=(0,0,0)$ (open rectangles), $\mathbf{r}=(0,a/2,a/2)$ (open circles), $\mathbf{r}=(a/2,0,a/2)$ (open triangles), and $\mathbf{r}=(a/2,a/2,0)$ (open diamonds) for the fcc lattice.

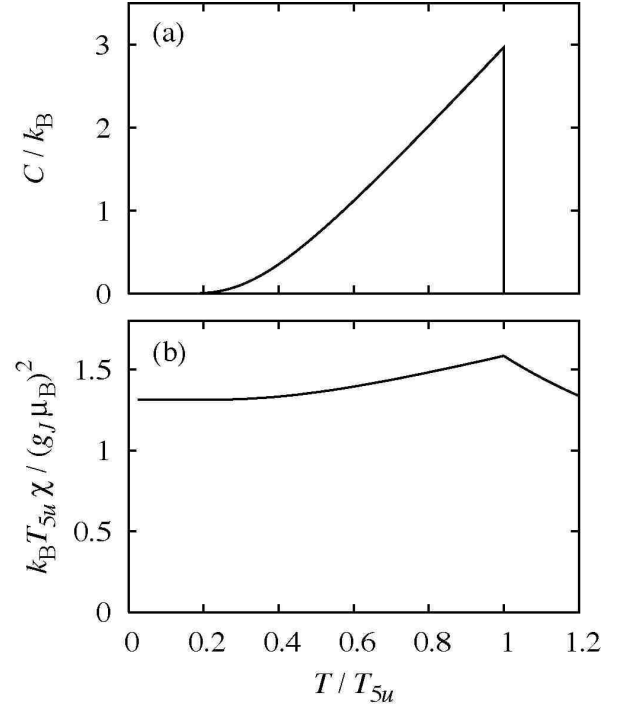


FIG. 10: Temperature dependence of physical quantities in the absence of a magnetic field for the fcc lattice. (a) Specific heat. (b) Magnetic susceptibility.

sion of Γ_7 orbital in our model. The analysis of the $j=5/2$ sextet model on the fcc lattice is one of future problems.

V. DISCUSSION AND SUMMARY

We have constructed Γ_8 models with hopping integrals through ($ff\sigma$) bonding based on the j - j coupling scheme. In order to study multipole ordering, we have derived an effective model by using the second-order perturbation theory with respect to f - f hopping. By applying mean-field theory, we find different multipole ordered states depending on the lattice structure. For the sc lattice, a Γ_{3g} antiferro-quadrupole transition occurs at a finite temperature. As lowering temperature further, we find a ferromagnetic transition. For the bcc lattice, a Γ_{2u} antiferro-octupole ordering occurs first, and a ferromagnetic transition follows it. Finally, for the fcc lattice, with careful analysis, we conclude the appearance of the single phase transition to the triple- \mathbf{q} Γ_{5u} octupole ordering.

In this paper, we have not taken into account the effect of conduction electron. One may complain about this point, since it is believed that the hybridization of f electrons with conduction electron band is important to understand the magnetism of f -electron systems. In fact, in the traditional prescription, first we derive the Coqblin-Schrieffer model from the periodic Anderson model by evaluating the c - f exchange interaction J_{cf} within the second-order perturbation in terms of the hybridization between f - and conduction electrons.⁴⁰ Then, we derive the RKKY interactions again using the second-order perturbation theory with respect to J_{cf} .

In general, the RKKY interactions are orbital dependent and interpreted as multipole interactions. Such orbital dependence originates from that of the hybridization. Note that the hybridization should occur only between f - and conduction band with the same symmetry. Here we emphasize that the symmetry of f -electron state is correctly included in our calculations. Thus, the structure in the multipole interactions will not be changed so much, even if we consider the effect of hybridization with conduction band, as long as we consider correctly the symmetry of f electron states.

Let us show an example to support our belief. Concerning the octupole ordering in NpO_2 , we have extended the present theory by further including the effect of p electrons of oxygen anions.³³ Namely, we have constructed the so-called f - p model, given in the form of

$$\mathcal{H} = \mathcal{H}_f + \mathcal{H}_p + \mathcal{H}_{\text{hyb}}, \quad (35)$$

where \mathcal{H}_f and \mathcal{H}_p denote the local f - and p -electron terms, respectively, and \mathcal{H}_{hyb} is the hybridization between p - and f -electrons through ($pf\sigma$) and ($pf\pi$). Then, it has been found that the structure in the multipole interactions of the effective model derived from the f - p model is qualitatively the same as those obtained in the Γ_8 model on the fcc lattice. In fact, we have found a finite parameter region of Γ_{5u} antiferro-octupole phase. Namely, the f - p model on the fcc lattice has a tendency toward Γ_{5u} antiferro-octupole ordering, which has been already captured in the simple ($ff\sigma$) model. This result suggests that the structure in multipole interactions is determined mainly by the symmetry of f -electron state. Most of the effect of hybridization can be included by changing effectively ($ff\sigma$) in the multipole interactions shown in the present paper.

However, if the itinerant nature of f electrons is increased due to the large hybridization and metallicity of the ground state becomes significant, the present approximation inevitably loses the validity and the effect of the conduction band should be important. In such a case, it is necessary to develop a theory on the basis of the orbital-degenerate periodic Anderson model in order to include the multipole fluctuations. It is one of future tasks.

Acknowledgments

We thank M. Yoshizawa and H. Fukazawa for sending us preprints on $\text{SmRu}_4\text{P}_{12}$ prior to publication. We also thank H. Harima, S. Kambe, N. Metoki, Y. Tokunaga, K. Ueda, R. E. Walstedt, and H. Yasuoka for useful discussions. One of the authors (K. K.) is grateful to H. Onishi for useful comments on numerical diagonalization. K. K. is supported by the REIMEI Research Resources of Japan Atomic Energy Research Institute. Another author (T. H.) is supported by a Grants-in-Aid for Scientific Research in Priority Area ‘‘Skutterudites’’ under the contract No. 16037217 from the Ministry of Education, Culture, Sports, Science, and Technology of Japan. T. H. is also supported by a Grant-in-Aid for Scientific Research (C)(2) under the contract No. 50211496 from Japan Society for the Promotion of Science.

¹ M. Imada, A. Fujimori, and Y. Tokura, Rev. Mod. Phys. **70**, 1039 (1998).

² Y. Tokura and N. Nagaosa, Science **288**, 462 (2000).

³ E. Dagotto, T. Hotta, and A. Moreo, Phys. Rep. **344**, 1 (2001).

⁴ T. Hotta and E. Dagotto, in *Colossal Magnetoresistive Manganites*, edited by T. K. Chatterji, p. 207, (Kluwer, Netherlands, 2004).

⁵ P. Santini, R. Lémanski, and P. Erdős, Adv. Phys. **48**, 537 (1999).

⁶ *Proceedings of the International Conference on Strongly Correlated Electrons with Orbital Degrees of Freedom*, J. Phys. Soc. Jpn. **71** (Suppl.) (2001).

⁷ Y. Kuramoto and H. Kusunose, J. Phys. Soc. Jpn. **69**, 671 (2000).

⁸ H. Kusunose and Y. Kuramoto, J. Phys. Soc. Jpn. **70**, 1751

- (2001).
- ⁹ T. Sakakibara, T. Tayama, K. Tenya, M. Yokoyama, H. Amitsuka, D. Aoki, Y. Ōnuki, Z. Kletowski, and S. Kunii, *J. Phys. Chem. Solids* **63**, 1147 (2002); T. Sakakibara, K. Tenya, and S. Kunii, *Physica B* **312-313**, 194 (2002); T. Morie, T. Sakakibara, T. Tayama, and S. Kunii, *J. Phys. Soc. Jpn.* **73**, 2381 (2004).
 - ¹⁰ K. Kubo and Y. Kuramoto, *J. Phys. Soc. Jpn.* **72**, 1859 (2003); **73**, 216 (2004).
 - ¹¹ S. Kobayashi, Y. Yoshino, S. Tsuji, H. Tou, M. Sera, and F. Iga, *J. Phys. Soc. Jpn.* **72**, 2947 (2003).
 - ¹² K. Iwasa, K. Kuwahara, M. Kohgi, P. Fischer, A. Dönni, L. Keller, T. C. Hansen, S. Kunii, N. Metoki, Y. Koike, and K. Ohoyama, *Physica B* **329-333**, 582 (2003).
 - ¹³ O. Suzuki, S. Nakamura, M. Akatsu, Y. Nemoto, T. Goto, and S. Kunii, *J. Phys. Soc. Jpn.* **74**, 735 (2005).
 - ¹⁴ P. Santini and G. Amoretti, *Phys. Rev. Lett.* **85**, 2188 (2000); *J. Phys. Soc. Jpn.* **71** (Suppl.), 11 (2002).
 - ¹⁵ J. A. Paixão, C. Detlefs, M. J. Longfield, R. Caciuffo, P. Santini, N. Bernhoeft, J. Rebizant, and G. H. Lander, *Phys. Rev. Lett.* **89**, 187202 (2002); R. Caciuffo, J. A. Paixão, C. Detlefs, M. J. Longfield, P. Santini, N. Bernhoeft, J. Rebizant, and G. H. Lander, *J. Phys.: Condens. Matter* **15**, S2287 (2003).
 - ¹⁶ S. W. Lovesey, E. Balcar, C. Detlefs, G. van der Laan, D. S. Sivia, and U. Staub, *J. Phys.: Condens. Matter* **15**, 4511 (2003).
 - ¹⁷ A. Kiss and P. Fazekas, *Phys. Rev. B* **68**, 174425 (2003).
 - ¹⁸ Y. Tokunaga, Y. Homma, S. Kambe, D. Aoki, H. Sakai, E. Yamamoto, A. Nakamura, Y. Shiokawa, R. E. Walstedt, and H. Yasuoka, *Phys. Rev. Lett.* **94**, 137209 (2005).
 - ¹⁹ O. Sakai, R. Shiina, and H. Shiba, *J. Phys. Soc. Jpn.* **74**, 457 (2005).
 - ²⁰ K. Kubo and T. Hotta, *Phys. Rev. B* **71**, 140404(R) (2005).
 - ²¹ M. Yoshizawa, Y. Nakanishi, M. Oikawa, C. Sekine, I. Shiro-tani, S. R. Saha, H. Sugawara, and H. Sato, preprint.
 - ²² K. Hachitani, H. Fukazawa, Y. Kohori, I. Watanabe, C. Sekine, and I. Shiro-tani, preprint.
 - ²³ E. Zirngiebl, B. Hillebrands, S. Blumenröder, G. Güntherodt, M. Loewenhaupt, J. M. Carpenter, K. Winzer, and Z. Fisk, *Phys. Rev. B* **30**, 4052 (1984); N. Sato, S. Kunii, I. Oguro, T. Komatsubara, and T. Kasuya, *J. Phys. Soc. Jpn.* **53**, 3967 (1984); B. Lüthi, S. Blumenröder, B. Hillebrands, E. Zirngiebl, G. Güntherodt, and K. Winzer, *Z. Phys. B* **58**, 31 (1984).
 - ²⁴ J. M. Fournier, A. Blaise, G. Amoretti, R. Caciuffo, J. Larroque, M. T. Hutchings, R. Osborn, and A. D. Taylor, *Phys. Rev. B* **43**, 1142 (1991); G. Amoretti, A. Blaise, R. Caciuffo, D. Di Cola, J. M. Fournier, M. T. Hutchings, G. H. Lander, R. Osborn, A. Severing, and A. D. Taylor, *J. Phys.: Condens. Matter* **4**, 3459 (1992).
 - ²⁵ K. Matsuhira, Y. Hinatsu, C. Sekine, T. Togashi, H. Maki, I. Shiro-tani, H. Kitazawa, T. Takamasu, and G. Kido, *J. Phys. Soc. Jpn.* **71** (Suppl.), 237 (2002); M. Yoshizawa, Y. Nakanishi, T. Kumagai, M. Oikawa, C. Sekine, and I. Shiro-tani, *J. Phys. Soc. Jpn.* **73**, 315 (2004); K. Matsuhira, Y. Doi, M. Wakeshima, Y. Hinatsu, H. Amitsuka, Y. Shimaya, R. Giri, C. Sekine, and I. Shiro-tani, *J. Phys. Soc. Jpn.* **74**, 1030 (2005).
 - ²⁶ R. Shiina, H. Shiba, and P. Thalmeier, *J. Phys. Soc. Jpn.* **66**, 1741 (1997).
 - ²⁷ D. Schmitt and P. M. Levy, *J. Magn. Magn. Mater.* **49**, 15 (1985).
 - ²⁸ G. Sakurai and Y. Kuramoto, *J. Phys. Soc. Jpn.* **73**, 225 (2004); **74**, 975 (2005).
 - ²⁹ T. Hotta and K. Ueda, *Phys. Rev. B* **67**, 104518 (2003).
 - ³⁰ T. Hotta, *Phys. Rev. B* **70**, 054405 (2004).
 - ³¹ T. Hotta, *Phys. Rev. Lett.* **94**, 067003 (2005).
 - ³² T. Hotta, *J. Phys. Soc. Jpn.* **74**, 1275 (2005).
 - ³³ K. Kubo and T. Hotta, cond-mat/0505548.
 - ³⁴ K. Takegahara, Y. Aoki, and A. Yanase, *J. Phys. C: Solid St. Phys.* **13**, 583 (1980).
 - ³⁵ O. Sakai, R. Shiina, and H. Shiba, *J. Phys. Soc. Jpn.* **72**, 1534 (2003).
 - ³⁶ P. W. Anderson, *Phys. Rev.* **115**, 2 (1959).
 - ³⁷ K. I. Kugel and D. Khomskii, *Sov. Phys. JETP* **37**, 725 (1973).
 - ³⁸ J. van den Brink, P. Horsch, F. Mack, and A. M. Oleś, *Phys. Rev. B* **59**, 6795 (1999); K. Kubo, *J. Phys. Soc. Jpn.* **71**, 1308 (2002).
 - ³⁹ J. W. Ross and D. J. Lam, *J. Appl. Phys.* **38**, 1451 (1967); P. Erdős, G. Solt, Z. Zolnierrek, A. Blaise, and J. M. Fournier, *Physica B & C* **102B**, 164 (1980).
 - ⁴⁰ B. Coqblin and J. R. Schrieffer, *Phys. Rev.* **185**, 847 (1969).